Reduced Molybdenum-Niobium Oxides. 1. Synthesis, Structure, and Physical Properties of $K_2Mo_4Nb_3O_{20}$

S. C. Chen, B. Wang, and M. Greenblatt*

Department of Chemistry, Rutgers, The State University of New Jersey, Piscataway, New Jersey 08855-0939

Received March 24, 1993®

$K_2Mo_4Nb_3O_{20}$ crystallizes in the orthorhombic system, space group *Pbcm* (No. 57). The unit cell dimensions are $a = 4.0176(7)$ Å, $b = 17.891(4)$ Å, $c = 21.825(3)$ Å, $V = 1568.7(5)$ Å^3, and $Z = 4$. Because of the inability to distinguish between the Mo and Nb atoms by X-ray diffraction, the structure of $K_2Mo_4Nb_3O_{20}$ was refined on the basis of $K_2Mo_7O_{20}$. The final residual indexes are $R = 0.035$ and $R_w = 0.041$, with 717 observed reflections ($I > 3\sigma(I)$) and 98 variable parameters. The structure of $K_2Mo_4Nb_3O_{20}$ consists of pentagonal clusters of polyhedra that are linked together via bridging, corner-sharing octahedra in the *bc* plane. These layers stack along the *a* axis, forming pentagonal columns and octahedral strings. The pentagonal cluster of polyhedra contains an MO_7 pentagonal bipyramid that shares equatorial edges with five MO_6 octahedra, forming a star-shaped cluster of polyhedra (M = Mo, Nb). The K ions are located in the one-dimensional S-shaped tunnels, running along the *a* axis, created by the network of polyhedra. $K_2Mo_4Nb_3O_{20}$ is an electronic insulator and exhibits ionic conductivity at temperature above 150 °C. The temperature dependence of the magnetic susceptibility of $K_2Mo_4Nb_3O_{20}$ does not follow Curie-Weiss behavior. A magnetic moment of 1.56 μ_B/mol calculated at 250 K is consistent with one localized electron per formula unit estimated from the valence count.

Introduction

The ternary bronzes of transition metals have been of interest since the discovery of the tungsten bronzes, Na_xWO_3, by Wohler.[1] The alkali metal tungsten bronzes, A_xWO_3 ($0.0 < x < 1.0$), have been studied most intensively and reviewed in the past.[2-5] Recently, interest in the transition metal bronzes has focused on the study of the molybdenum bronzes due to their quasi-low-dimensional properties, which include highly anisotropic transport properties, charge density wave (CDW) driven metal-to-semiconductor transition, and superconductivity, as described in several reviews.[6-8] In contrast to the numerous compounds of ternary W or Mo bronzes, there are only a few ternary Ta[9] or Nb[10] bronzes reported.

The structures of ternary W bronzes are quite different from those of Mo bronzes. The ternary tungsten bronzes, characterized by their nonstoichiometric compositions, have three dimensional structures built up from corner-sharing WO_6 octahedra.[11] The ternary molybdenum bronzes, on the other hand, are typically layered compounds with edge/corner-sharing MoO_6 octahedra.[6] Similar structural preference was also observed in the ternary bronzes of Ta and Nb; $BaTa_2O_5$ crystallizes in a hexagonal system[9] whereas the structures of A_xNbO_3 (A = Sr, Ba) are tetragonal (I) tungsten bronze (TTB) type for $0.6 < x < 0.7$ and cubic perovskite for $0.7 < x < 0.95$.[10] Interestingly, the high pressure prepared A_xMoO_3 (A = K, Rb) compounds are known to be isostructural with their W analogues.[12]

Despite of the rich chemistry of ternary bronzes, little is known about the reduced quaternary oxides of the type $A_nM_xM'_yO_z$, where A could be any alkali or rare earth metal, M = Nb, Ta and M' = Mo, W. We have previously reported a quaternary Mo-Nb bronze $K_{5.3}Mo_{9.2}Nb_{0.8}O_{30}$, the first example of a molybdenum bronze prepared at low pressure with a TTB-type structure.[13] The Mo atoms occupy the octahedral sites and the Nb atoms are situated in the trigonal tunnels of the TTB structure of $K_{5.3}Mo_{9.2}Nb_{0.8}O_{30}$, while the K atoms are located in pentagonal and square tunnels. The structural ordering of the Mo and Nb atoms and their partial occupancies suggest that the Nb atoms play an important role in the stabilization of molybdenum bronzes with the TTB-type structure. Here we report the synthesis, structure, and physical properties of a new reduced quaternary Mo-Nb oxide—$K_2Mo_4Nb_3O_{20}$.

Experimental Section

Materials. Prior to use, K_2CO_3 (Aldrich, 99+%) was dried at 300 °C for 1 h, Nb_2O_5 (Alfa Product, 99.5%) at 1100 °C for 9 h, and MoO_3 (Johnson Matthey, 99.95%) at 550 °C for 9 h in air. K_2MoO_4 was prepared by the reaction of K_2CO_3 with a stoichiometric amount of MoO_3 in an alumina crucible at 550 °C for 15 h in air. Mo (Alfa Products, -100 mesh, 99.7%), MoO_2 (Alfa Products, 99%) and NbO_2 (Alfa Products, 99+%) were used as obtained without any further purification.

Synthesis. In a reaction designed to prepare polycrystalline single phase $K_{5.3}Mo_{9.2}Nb_{0.8}O_{30}$,[13] a mixture containing stoichiometric amounts of K_2MoO_4, MoO_3, Nb_2O_5 and Mo was thoroughly mixed, put in a platinum boat, and then sealed in a quartz tube under a dynamic vacuum. The reaction mixture was fired at 1100 °C for 3 days. Black plate-like crystals were discovered in the platinum boat. The stoichiometry of these crystals was later estimated as $K_2M_7O_{20}$ (M = Mo, Nb) by qualitative elemental analysis and X-ray crystallographic studies.

* To whom correspondence should be addressed.

® Abstract published in *Advance ACS Abstracts*, September 1, 1993.

(1) Wohler, F. *Philos. Mag.* **1825**, *66*, 263. (English translation)
(2) Banks, E.; Wold, A. *Preparative Inorganic Reactions*; Jolly, W. L., Ed.; Interscience: New York, 1968; Vol. 4, p 237.
(3) Hagenmuller, P. *Progress in Solid State Chemistry*; Reiss, H., Ed.; Pergamon: New York, 1971; Vol. 5, p 71.
(4) Sienko, M. J. *Nonstoichiometric Compounds*; Gould, R. F., Ed.; Advances in Chemistry 39; American Chemical Society: Washington, DC, 1963; p 224.
(5) Dickens, P. G.; Whittingham, M. S. *Q. Rev., Chem. Soc.* **1968**, *22*, 30.
(6) Manthiram, A.; Gopalakrishnan, J. *Rev. Inorg. Chem.* **1984**, *6*, 1.
(7) Greenblatt, M. *Chem. Rev.* **1988**, *88*, 31.
(8) Schlenker, C. *Low-Dimensional Electronic Properties of Molybdenum Bronzes and Oxides*; Kluwer Academic Publishers: Boston, MA, 1989.
(9) Galasso, F. S.; Katz, L.; Ward, R. *J. Am. Chem. Soc.* **1958**, *80*, 1262.
(10) (a) Ridgley, D.; Ward, R. *J. Am. Chem. Soc.* **1955**, *77*, 6132. (b) Sunshine, S. A.; Hessen, B.; Siegrist, T.; Fiory, A. T.; Waszczak, J. V. *Chemistry of Electronic Ceramic Materials*; National Institute of Standards and Technology Special Publication 804; Proceedings of the International conference held in Jackson, WY, August 17-22, 1990; NIST: Washington, DC, 1991. (c) Hessen, B.; Sunshine, S. A.; Siegrist, T.; Jimenez, R. *Mater. Res. Bull.* **1991**, *26*, 85.
(11) (a) Brown, B. W.; Banks, E. *J. Am. Chem. Soc.* **1954**, *76*, 963. (b) Magneli, A.; Blomberg, B. *Acta Chem. Scand.* **1951**, *5*, 375.
(12) Bither, T. A.; Gillson, J. L.; Young, H. S. *Inorg. Chem.* **1966**, *5*, 1559.
(13) Chen, S. C.; Greenblatt, M. *J. Solid State Chem.* **1993**, *104*, 353.

0020-1669/93/1332-4306$04.00/0

In attempts to prepare single-phase polycrystalline $K_2Mo_{7-x}Nb_xO_{20}$ ($x = 0, 1, 2$, and 3), reaction mixtures containing K_2MoO_4, MoO_3, MoO_2, NbO_2, and Nb_2O_5 in molar ratios of 1:4:2:0:0 for $x = 0$, 1:4:1:1:0 for $x = 1$, 1:4:0:2:0 for $x = 2$, and 1:3:0:1:1 for $x = 3$ were each mixed together thoroughly and pelletized. Each of these pellets was then put in a gold boat and sealed in a quartz tube under a dynamic vacuum. Samples were first held at 500 °C for 2 days to react the volatile MoO_3 and then at 700–900 °C for another 2–3 days. A single-phase X-ray powder pattern was observed only for the $x = 3$ member, $K_2Mo_4Nb_3O_{20}$, at 700–750 °C. Diffraction lines corresponding to $K_2Mo_{7-x}Nb_xO_{20}$ and MoO_2 were always observed in reactions corresponding to $x = 1$ and 2. Attempts at the preparation of the $x = 0$ member always resulted in a mixture of blue bronze ($K_{0.3}MoO_3$, crystals), red bronze ($K_{0.33}MoO_3$), and MoO_2. A similar synthetic approach with Mo as the reducing agent was also tried, but gave similar results. The purity of samples was monitored by powder X-ray diffraction with a SCINTAG PAD V diffractometer using filtered Cu Kα radiation.

Single-Crystal X-ray Crystallographic Studies. A rectangular platelike crystal having approximate dimensions of $0.18 \times 0.03 \times 0.01$ mm^3 was selected for both elemental analysis and single-crystal X-ray crystallographic study. The qualitative elemental analysis on a single crystal with an electron microprobe (JEOL 8600 Superprobe) indicated the presence of K, Mo, and Nb. The preliminary lattice parameters were determined from oscillation and Weissenberg photographs. The final unit cell parameters were determined from least-squares analysis of the setting angles of 25 chosen reflections in the range $33° < 2\theta < 44°$ automatically centered on an Enraf-Nonius CAD4 diffractometer. The intensity data were collected at room temperature. Graphite-monochromated Mo Kα radiation was employed to collect data with $4° \le 2\theta \le 50°$. A ω–2θ scan mode was used. Three standard reflections measured every 2 h showed no apparent decay in intensity in the course of data collection. The intensity data was corrected for Lorentz polarization effects. Because of the highly distorted (Mo, Nb)O_6 octahedra and the similar scattering factors of Nb and Mo, the Nb and Mo atoms are indistinguishable in the structural refinement. The structure was thus refined on the model of $K_2Mo_7O_{20}$. The linear absorption coefficient for Mo Kα is 59.5 cm^{-1}, based on the $K_2Mo_7O_{20}$ model. A Gaussian absorption correction was applied after measuring the crystal faces.[14] The correction factors were in the range 0.859–0.943. In the octant (h, k, l), 1413 unique reflections were collected, of which 717 reflections with $I > 3\sigma(I)$ were considered as observed and used in the subsequent structural solution and refinement.

The systematic absences ($0kl$, $k \neq 2n$; $h0l$, $l \neq 2n$; $0k0$, $k \neq 2n$; and $00l$, $l \neq 2n$) reduced the possible space groups to *Pbcm* (No. 57) and $Pca2_1$ (No. 29). The structure was solved by direct methods (SHELXS-86)[15] in the centrosymmetric space group *Pbcm* and refined on $|F|$ by using the full-matrix least-square techniques in the MolEN program package.[16] On the basis of 717 reflections and 98 variable parameters, the structure was anisotropically refined to $R = 0.035$, $R_w = 0.041$, and $R_{(zero)} = 0.1440$ with 10 of the 12 oxygen atoms isotropically refined. Our inability to refine all the oxygen atoms anisotropically presumably originates from the low observed reflection-to-parameter ratio (~7:1). The refinement of the multiplicities of K ($B_{eq} = 2.9(1)$ Å^2) and O(3) ($B_{eq} = 1.5(2)$ Å^2) atoms showed no sign of partial occupancies. The final electron density difference map was flat with a maximum of 1.3 e/Å^3 close to O(11) and a minimum of –1.3 e/Å^3 close to O(1). A similar model in the noncentrosymmetric space group $Pca2_1$ (No. 29) was also tested, but converged very slowly to a larger R_w, and, hence, does not represent an improvement versus space group *Pbcm* (No. 57).

Selected X-ray crystallographic data of $K_2M_7O_{20}$ (M = Mo, Nb) are presented in Table I. The final positional and isotropic thermal parameters of atoms are given in Table II. Selected bond distances are listed in Table III.

Physical Properties Measurements. Single-phase $K_2Mo_4Nb_3O_{20}$ powder was ground, pressed into two pellets, put in a gold boat, vacuum sealed in a quartz tube, and sintered at 700 °C for 1 day. These two pellets were later used for physical properties measurements. A SQUID magnetometer (MPMS, Quantum Design) was used for the magnetic susceptibility measurements in the temperature range 4–250 K at an applied field of 1000 G. The room-temperature resistivity was measured by a standard four-probe technique with a DE 202 Cryostat (APD cryogenics). A sintered pressed disk was coated with platinum paste on the two opposite faces and dried in an oven (160 °C) for 3 h, before making the ionic conductivity measurements. Ionic conductivities were measured by the ac complex impedance technique under argon atmosphere. A Solartron Model 1250 frequency analyzer and an Model 1186 electrochemical interface programmed by a Hewlett-Packard 9816 desktop computer were used for data collection and analysis. The frequency range applied was 10 Hz to 65 kHz. The heating rate was 2 °C/min in the temperature range 150–400 °C. Powder X-ray diffraction verified that single-phase $K_2Mo_4Nb_3O_{20}$ was still present after the ionic conductivity measurements.

Table I. Crystallographic Data for $K_2M_7O_{20}$ (M = Mo, Nb)[a]

empirical formula	$K_2Mo_7O_{20}$	fw	1069.77
space group	*Pbcm* (No. 57)	T, °C	20
a, Å	4.0176(7)	λ, Å	0.710 69
b, Å	17.891(4)	d_{calcd}, g/cm^3	4.53
c, Å	21.825(3)	μ (Mo Kα), cm^{-1}	59.5
V, Å^3	1568.7(5)	R^b	0.035
Z	4	R_w^c	0.041

[a] Data reported are based on the refined model of $K_2Mo_7O_{20}$. [b] $R = \sum||F_o| - |F_c||/\sum|F_o|$. [c] $R_w = [\sum w(|F_o| - |F_c|)^2/\sum w|F_o|^2]^{1/2}$; $w = 1/(\sigma^2|F_o|)$.

Table II. Atomic Coordinates and B_{eq}[a] for $K_2M_7O_{20}$ (M = Mo, Nb)

atom	x	y	z	B_{eq}, Å^2
M(1)	0.0721(5)	0.29378(7)	0.66328(6)	0.42(2)
M(2)	0.0711(5)	0.41077(7)	0.39339(6)	0.47(2)
M(3)	0.0673(7)	0.750	0.500	0.63(4)
M(4)	0.0786(7)	0.6475(1)	0.750	0.48(3)
M(5)	0.0821(8)	0.5332(1)	0.250	0.67(4)
K	0.501(1)	0.5911(3)	0.0527(3)	2.9(1)
O(1)	0.502(3)	0.2948(6)	0.6626(5)	1.1(2)[b]
O(2)	0.005(3)	0.0032(6)	0.5737(5)	1.0(3)
O(3)	0.505(3)	0.0934(7)	0.6096(6)	1.5(2)[b]
O(4)	0.998(3)	0.3016(6)	0.5796(5)	0.7(2)[b]
O(5)	0.997(3)	0.4450(6)	0.1930(5)	0.8(2)[b]
O(6)	0.997(3)	0.1513(6)	0.5390(5)	0.6(3)
O(7)	0.496(4)	0.250	0.500	0.6(3)[b]
O(8)	0.997(3)	0.3931(5)	0.6869(5)	0.5(2)[b]
O(9)	0.984(4)	0.2629(8)	0.750	0.4(3)[b]
O(10)	0.506(4)	0.9668(8)	0.750	0.5(3)[b]
O(11)	0.985(3)	0.1837(5)	0.6610(4)	0.3(2)[b]
O(12)	0.483(4)	0.1464(7)	0.750	0.1(3)[b]

[a] $B_{eq} = {}^8/_3\pi^2\sum U_{ij}a_i^*a_j^*\mathbf{A}_i\mathbf{a}_j$, where the temperature factors are defined as $\exp(-2\pi^2\sum h_ih_ja_i^*a_j^*U_{ij})$. [b] Atoms were refined isotropically.

Table III. Selected Interatomic Distance (Å) for $K_2M_7O_{20}$ (M = Mo, Nb)

M(1)–O(1)	2.29(1)	M(4)–O(5)	2.09(1) × 2[a]
M(1)–O(1)	1.73(1)	M(4)–O(9)	2.08(2)
M(1)–O(4)	1.86(1)	M(4)–O(11)	2.06(2) × 2[a]
M(1)–O(8)	1.87(1)	M(4)–O(12)	2.26(2)
M(1)–O(9)	2.004(5)	M(4)–O(12)	1.76(2)
M(1)–O(11)	2.00(1)	M(5)–O(5)	2.04(1) × 2[a]
M(2)–O(2)	1.72(1)	M(5)–O(8)	1.93(1) × 2[a]
M(2)–O(3)	2.28 (1)	M(5)–O(10)	2.31(2)
M(2)–O(3)	1.75(1)	M(5)–O(10)	1.70(2)
M(2)–O(5)	2.00(1)	K–O(1)	3.15(1)
M(2)–O(6)	1.87(1)	K–O(2)	2.65(1)
M(2)–O(11)	2.09(1)	K–O(2)	2.67(1)
M(3)–O(4)	1.99(1) × 2[a]	K–O(4)	2.84(1) × 2[a]
M(3)–O(6)	1.98(1) × 2[a]	K–O(6)	3.03(1) × 2[a]
M(3)–O(7)	2.26(2)	K–O(7)	3.066(5)
M(3)–O(7)	1.75(2)		
K···K	3.990(2)[b]	O(2)···O(4)	3.608(2)[d]
K···K	4.018(2)[c]	O(2)···O(6)	3.700(2)[d]

[a] Indicates the number of bonds of this distance and type. [b] Nonbonding distance within the same S-shaped tunnel. [c] Nonbonding distance between the neighboring S-shaped tunnels. [d] Nonbonding distances.

Results and Discussion

Structure. The structure of $K_2Mo_4Nb_3O_{20}$ is discussed based on $K_2M_7O_{20}$ (M = Mo, Nb), which is isostructural with the fully

(14) Coppens, P.; Leiserowitz, L.; Rabinovich, D. *Acta Crystallogr.* **1965**, *18*, 1035.
(15) Sheldrick, G. M. In *Crystallographic Computing 3*; Sheldrick, G. M., Kruger, C., Goddar, R., Eds.; Oxford University Press: London, 1985; pp 175–189.
(16) Fair, C. K. *MolEN*; Enraf-Nonius, Delft Instruments X-Ray Diffraction B.V.: Delft, The Netherlands, 1990.

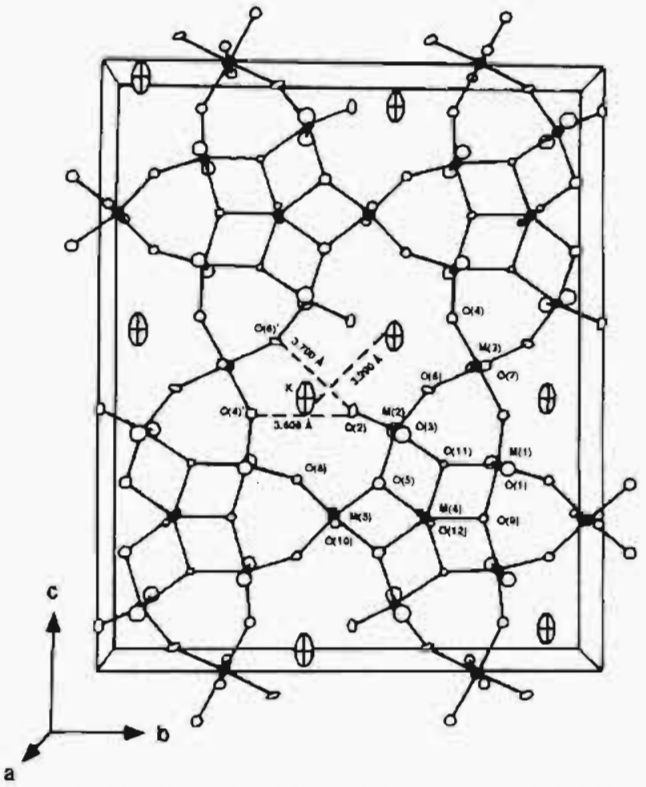

Figure 1. ORTEP drawing (50% thermal ellipsoids) of the unit cell structure of $K_2M_7O_{20}$ (M = Mo, Nb), viewing along the *a* axis. The thermal ellipsoids of O(12) have been enlarged by a factor of 2 for clarity.

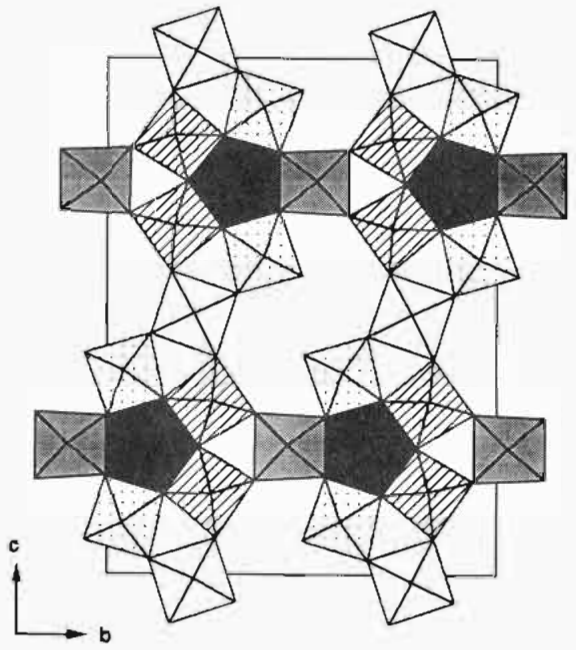

Figure 2. Polyhedral representation of the unit cell structure of $K_2M_7O_{20}$ (M = Mo, Nb), viewing along the *a* axis. The striped, dotted, blank, and shaded octahedra represent $M(1)O_6$, $M(2)O_6$, $M(3)O_6$, and $M(5)O_6$, respectively. $M(4)O_7$ is represented by the shaded pentagonal bipyramids. The K atoms are not shown.

oxidized compound $Na_7Nb_{15}W_{13}O_{80}$.[17] The ORTEP drawing and polyhedral representation of the unit cell structure of $K_2M_7O_{20}$ (M = Mo, Nb) viewed along the *a* axis are presented in Figures 1 and 2, respectively. The structure consists of two types of building polyhedra: MO_7 pentagonal bipyramids and MO_6 octahedra (M = Mo, Nb). Each pentagonal bipyramid ($M(4)O_7$) is linked by equatorial edge-sharing to five octahedra forming a star-shaped cluster of polyhedra (Figure 2). Along the *b* axis, the star-shaped clusters of polyhedra are coupled together *via* triangular links (O(8)–O(9)–O(8)') in a manner found in the structures of $M_xNb_6(O, F)_{16}$ (M = Li, Na, Mn, Cu, and Cd),[18] M_2WO_8 (M = Nb and Ta),[19] $Cu_{0.8}Ta_3O_8$[20] and the high-temperature form of $LiTa_3O_8$[21] and Ta_3O_7F.[22] Along the *c* axis, the clusters of polyhedra are connected via corner-sharing with a $M(3)O_6$ octahedron. The star-shaped clusters of polyhedra are stacked on top of one another through apical-sharing forming pentagonal columns (PC) running parallel to the *a* axis. Likewise, the bridging $M(3)O_6$ octahedra corner-share to form strings running parallel to the a axis. The tunnels created by this network of polyhedra are S-shaped in cross section and run along the *a* axis. The K ions are located in these tunnels (Figure 1).

It is worth noting that the pentagonal column (PC) structural units have also been observed in the structures of numerous fully oxidative forms of Nb[18,23] and Ta[20-22,24] oxides and oxyfluorides, as well as their W-doped analogs.[19,25] However, observation of PC in reduced oxides of the group V and VI transition metals are rare and, to the best of our knowledge, only seen in the compounds Mo_5O_{14}, $Mo_{17}O_{47}$,[26] $W_{18}O_{49}$, and $W_{24}O_{68}$.[27] The connectivity of the PC units vary from compound to compound and the tunnels created are rich in their shapes, ranging from trigonal to S-shaped. For example, in addition to the S-shaped tunnels reported here, V-shaped and regular heptagonal tunnels were observed in $Mo_{17}O_{47}$[26] and $TlNb_7O_{18}$,[23b] respectively. A review on the geometry of PC and its compatibility with the ReO_3-type structure was given by Marinder.[28]

Unlike the relatively regular polyhedra observed in the compounds mentioned above, the $M(4)O_7$ and MO_6 (M = Mo or Nb) polyhedra observed in $K_2M_7O_{20}$ (M = Mo, Nb) are highly distorted along the shortest axis, as also observed in $Na_7Nb_{15}W_{13}O_{80}$.[17] As shown in Table I and Figure 1, the distortion of polyhedra arises from the fact that the M atoms are displaced from $x = 0.0$ and the O atoms are less than 3σ from $z = 0.0$ or 0.5. Similar positional displacements were also observed in $Na_7Nb_{15}W_{13}O_{80}$,[17] Nb_2WO_8[19a] and $Na_3Nb_{12}O_{31}F$;[23a] however, the reason for this is not clear yet. It was commonly observed that the MO_6 octahedra are much more distorted than the MO_7 pentagonal bipyramids in compounds containing PC.[21-27] The M(4)–O distances of the pentagonal bipyramid in $K_2M_7O_{20}$ (M = Mo, Nb) are between 1.76(2) and 2.26(2) Å. The octahedra in $K_2M_7O_{20}$ (M = Mo, Nb) have M–O bond distances in the range 1.73(1)–2.29(1) Å for $M(1)O_6$, 1.72(1)–2.28(1) Å for $M(2)O_6$, 1.75(2)–2.26(2) Å for the bridging $M(3)O_6$, and 1.70(2)–2.31(2) Å for $M(5)O_6$. Similar distorted MoO_6 octahedra were previously observed in MoO_3 and other molybdenum oxides with the oxidation number of Mo close to 6.[6] For example, the Mo–O bond distances of the MoO_6 octahedron in MoO_3 fall into the range 1.67–2.33 Å (average 1.98 Å).[6] The relatively long distances observed for the M(4)–O bond (average 2.06 Å) in a pentagonal bipyramid compared to those (average 1.95–1.99 Å)

(17) Marinder, B. O.; Sundberg, M. *Acta Crystallogr.* **1984**, *C40*, 1303.

(18) (a) Lundberg, M. *Acta Chem. Scand.* **1965**, *19*, 2274. (b) Andersson, S. *Acta Chem. Scand.* **1965**, *19*, 2885. (c) Krumeich, F.; Gruehn, R. *Z. Anorg. Allg. Chem.* **1990**, *580*, 95. (d) Krumeich, F.; Gruehn, R. *Z. Anorg. Allg. Chem.* **1990**, *585*, 105.

(19) (a) Lundberg, M. *Acta Chem. Scand.* **1972**, *26*, 2932. (b) Santoro, A.; Roth, R. S.; Minor, D. *Acta Cryst.* **1979**, *B35*, 1202.

(20) Wa Hunga, P. N.; Marinder, B. O.; Lundberg, M. *Chem. Scr.* **1981**, *18*, 217.

(21) Nord, A. G.; Thomas, J. O. *Acta Chem. Scand.* **1978**, *A32*, 539.

(22) Jahnberg, L.; Andersson, S. *Acta Chem. Scand.* **1967**, *21*, 615.

(23) (a) Li, D. X. *J. Solid State Chem.* **1988**, *73*, 1. (b) Bhide, V.; Gasperin, M. *Acta Crystallogr.* **1979**, *B35*, 1318.

(24) Yamnova, N. A.; Pushcharovskii, D. Y.; Leonyuk, L. I.; Bogdanova, A. V. *Sov. Phys. Crystallogr.* **1988**, *33* (3), 358.

(25) Stephenson, N. C. *Acta Crystallogr.* **1968**, *B24*, 637.

(26) Kihlborg, L. *Ark. Kem.* **1963**, *21*, 471.

(27) (a) Sundberg, M. *Chem. Scr.* **1978–79**, *14*, 161. (b) Sahle, W.; Sundberg, M. *Chem. Scr.* **1980**, *16*, 163.

(28) Marinder, B.-O. *Angew. Chem., Int. Ed. Engl.* **1986**, *25*, 431.

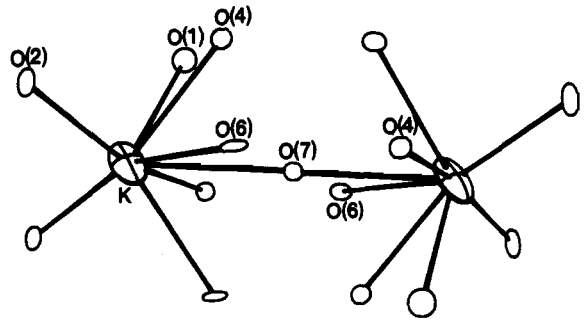

Figure 3. ORTEP drawing (50% thermal ellipsoids) of the coordination environment about the K atoms in $K_2M_7O_{20}$ (M = Mo, Nb). The two K atoms shown here are located at two neighboring S-shaped tunnels.

in octahedra can be understood from the fact that the coordination number of the M atoms is higher in $M(4)O_7$ than in MO_6. Interestingly, the average M–O distances of the octahedra that link the PC units are significantly longer than those of others; 1.99 Å for $M(3)O_6$ and $M(5)O_6$ compared to 1.95 Å for $M(1)O_6$ and $M(2)O_6$. This discrepancy in the bond distances might arise from differences in the structural rigidities around each octahedron.

A specific assignment of the Mo and Nb atoms to different polyhedral sites can not be made in $K_2M_7O_{20}$ (M = Mo, Nb) because of the highly distorted polyhedra and the inability to distinguish Mo from Nb by conventional X-ray diffraction techniques. The pentagonal bipyramidal and bridging octahedral sites in $Na_7Nb_{15}W_{13}O_{80}$, however, are almost entirely occupied by the Nb atoms.[17] This distribution of Nb implies that the pentagonal bipyramidal and bridging octahedral sites in $K_2Mo_4Nb_3O_{20}$ are most likely also occupied by the Nb atoms. Moreover, in $Na_7Nb_{15}W_{13}O_{80}$ the Nb and W atoms are disordered in the other octahedral sites.[17]

Figure 3 shows the coordination environment of the K atom. The K atom is eight-coordinated with the K–O bond distances in the range 2.65(1)–3.15(1) Å. The nonbonding distances of K–O in the S-shaped tunnel are 3.527 and 3.542 Å for K–O(3) and 3.567 Å for K–O(8). The K atoms located in the neighboring S-shaped tunnels are separated by 4.018(2) Å and linked together through the bridging oxygen (O(7)) at the apex of the $M(3)O_6$ octahedron. The K atoms in the same tunnel (Figure 1), on the other hand, are separated from one another by 3.990(2) Å.

Transport Properties. The room-temperature resistivity measurement on a pressed pellet, carried out by a standard four-probe technique, indicated that $K_2Mo_4Nb_3O_{20}$ is an electronic insulator with a room temperature resistivity in the order of 10^6 Ω cm. On the basis of the valence count, $K_2Mo_4Nb_3O_{20}$ has one electron in the 4d-manifold per molecule and would be expected to exhibit conducting behavior in view of its quasi-three-dimensional structure. However, due to the chemical difference between Mo and Nb, it is quite possible that the Mo and Nb atoms in $K_2Mo_4Nb_3O_{20}$ are structurally ordered in the framework of $K_2M_7O_{20}$ (M = Mo, Nb). This possible structural ordering of Mo and Nb can not be detected by conventional X-ray diffraction, but could be seen by neutron diffraction or by synchrotron X-ray diffraction, using anomalous dispersion effects. Structural ordering of Mo and Nb in this compound is consistent with the ordering of W and Nb in isostructural $Na_7Nb_{15}W_{13}O_{80}$ as discussed above. Such ordering of the Mo and Nb atoms in $K_2Mo_4Nb_3O_{20}$ would create potential electron traps and hinder the flow of the conducting electrons, giving an observed insulating behavior. A similar insulating behavior was also observed in the room-temperature resistivity measurement on a single crystal of the reduced compound $(Mo, Nb)_{13}O_{33}$.[29]

AC impedance measurements revealed ionic conductivity of $K_2Mo_4Nb_3O_{20}$ in the temperature measured between 150 and

(29) Chen, S. C.; Greenblatt, M. *J. Solid State Chem.*, in press.

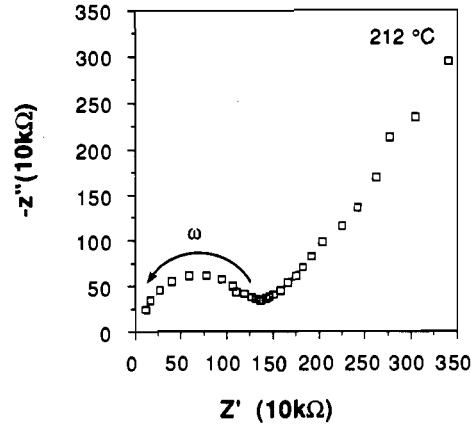

Figure 4. Ac complex impedance spectrum at 212 °C for $K_2Mo_4Nb_3O_{20}$.

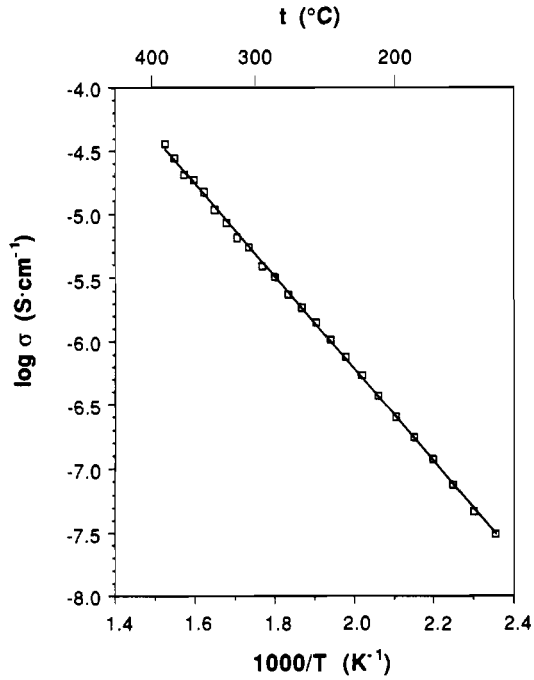

Figure 5. Arrhenius plot of ionic conductivity for $K_2Mo_4Nb_3O_{20}$.

400 °C. The relatively high isotropic temperature factor of the K atom (Table II) suggests the mobility of this ion. Figure 4 shows a typical AC impedance spectrum of $K_2Mo_4Nb_3O_{20}$ at 212 °C. The bulk (electrolyte) and the electrode–electrolyte effects are evident by the presence of a semicircle at higher frequencies and an inclined straight line at lower frequencies, respectively. Figure 5 displays the Arrhenius plot of the K^+ ion conductivity in $K_2Mo_4Nb_3O_{20}$. A linear behavior is observed in the measured temperature range 150–400 °C. The highest conductivity is 3.64×10^{-5} S cm^{-1} at 390 °C with E_a = 0.72 eV.

The low ionic conductivity of $K_2Mo_4Nb_3O_{20}$ is attributed to several interrelated factors that affect the conductivity: (1) the dimensionality of the structure, (2) the strength of the K^+–oxygen bonds, (3) the occupancy of the available K^+ sites, and (4) the size of the bottleneck for K^+ diffusion. As shown in Figure 1, the K^+ ions are situated in one dimensional S-shaped tunnels running along the *a* axis. The movement of the K^+ ions is thus expected to be mainly along this direction (i.e. one-dimensional). This structural low dimensionality limits K^+ movement and leads to the low ionic conductivities.

The K–O(2) bond distances of 2.65(1) and 2.67(1) Å (average 2.66 Å) in $K_2(Mo, Nb)_7O_{20}$ are significantly shorter than the covalent bond distance of K–O (K(VIII), 1.65 Å, and O(VI),

1.26 Å).[30] These strong K^+–oxygen bonds prevent the movement of the K^+ ions in $K_2Mo_4Nb_3O_{20}$.

One other factor with a significant influence on ionic conductivity is the degree of occupancy of the mobile ion site. In fast ionic conductors the mobile cations usually have partial occupancies of their sites. The full occupancy of K^+ ions in $K_2Mo_4Nb_3O_{20}$ is another factor that explains its low ionic conductivity.

The "bottleneck" size, i.e., the minimum opening in the structure that the mobile ions must pass through, is another important factor in ionic conductivity. The "bottlenecks" for K^+ diffusion along the *a* axis in $K_2M_7O_{20}$ (M = Mo, Nb), i.e., the narrowest regions in the tunnel, are only 3.608(2) and 3.700(2) Å for O(2)···O(4) and O(2)···O(6) distances, respectively (Figure 1). These bottleneck sizes are considerably smaller than the optimum size (5.5 Å) for K^+ ion diffusion, as suggested by Hong.[31] These small "bottlenecks" lead to a high activation energy (0.72 eV) and to a low ionic conductivity in $K_2Mo_4Nb_3O_{20}$.

Magnetic Properties. The molar magnetic susceptibility of $K_2Mo_4Nb_3O_{20}$ in the temperature region 4–250 K are presented in Figure 6. The magnetic moments were corrected for background (sample holder) and the diamagnetic core contributions. The observed magnetic susceptibility at 250 K is 1.22×10^{-3} emu/mol. On the basis of this value a moment of 1.56 μ_B is calculated for 1 mol of $K_2Mo_4Nb_3O_{20}$, which corresponds to one localized electron per formula unit of $K_2Mo_4Nb_3O_{20}$ and is consistent with that estimated from the valence count. The non-Curie–Weiss behavior observed in the plot of $1/\chi_m$ vs T suggests that electrons are not localized on lattice sites but are in narrow bands.

Conclusion

We have reported the synthesis and characterization of a new quaternary Mo–Nb oxide $K_2Mo_4Nb_3O_{20}$. $K_2Mo_4Nb_3O_{20}$ is an electronic insulator but exhibits weak ionic conductivity at temperatures above 150 °C. The magnetic moment calculated at 250 K is 1.56 μ_B/mol, corresponding to one localized electron per formula unit as estimated from the valence count. The non-Curie–Weiss behavior of the magnetic susceptibility of $K_2Mo_4Nb_3O_{20}$ suggests that electrons are localized in narrow bands, which is consistent with the observed insulating behavior.

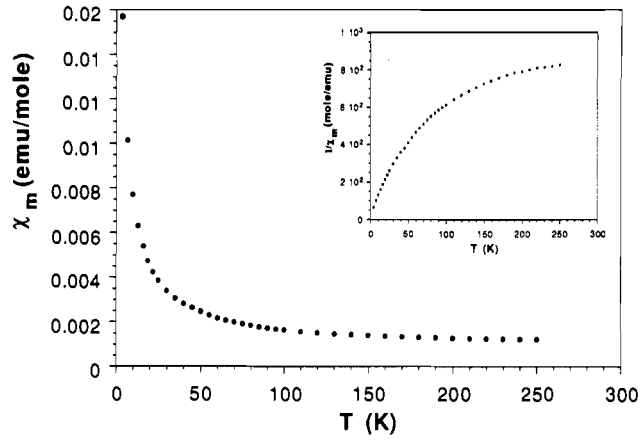

Figure 6. Variation of molar magnetic susceptibility with temperature for $K_2Mo_4Nb_3O_{20}$. The inset shows the variation of inverse susceptibility with temperature.

Acknowledgment. We thank Dr. K. V. Ramanujachary for helpful discussions of the physical properties of $K_2Mo_4Nb_3O_{20}$ and Professor W. H. McCarroll for critically reading the manuscript. We thank also Dr. Tom Emge for his assistances in the crystal structure determination. This work was supported by National Science Foundation Solid State Chemistry Grant DMR-90-19301.

Supplementary Material Available: Tables giving X-ray crystallographic details (Table SI), anisotropical thermal parameters (Table SII), interatomic distances (Table SIII) and angles (Table SIV) (6 pages). Ordering information is given on any current masthead page.

(30) Shannon, R. D. *Acta Crystallogr.* **1976**, *A32*, 751.
(31) Hong, H. Y-P. *Solid State Chemistry of Energy Conversion and Storage*; Goodenough, J. B., Whittingham, M. S., Eds.; American Chemical Society: Washington, DC, 1977; p 179.